MAKO: A high-performance, airborne imaging spectrometer for the long-wave infrared

D. W. Warren*, R. H. Boucher, D. J. Gutierrez, E. R. Keim, M. G. Sivjee
The Aerospace Corporation, P.O.Box 92957, Los Angeles, CA, USA 90009-2957

ABSTRACT

We report progress on a high-performance, long-wavelength infrared hyperspectral imaging system for airborne research. Based on a f/1.25 Dyson spectrometer and 128x128 arsenic doped silicon blocked impurity band array, this system has significantly higher throughput than previous sensors. An agile pointing/scanning capability permits the additional signal to be allocated between increased signal-to-noise and broader area coverage, creating new opportunities to explore LWIR hyperspectral phenomenology.

Keywords: spectrometer, hyperspectral, infrared, Dyson spectrometer

1. INTRODUCTION

The Dyson spectrometer form is well suited to compact, high throughput, dispersive hyperspectral sensors, such as are preferred for cryogenic space or airborne systems operating in the long wave infrared (LWIR) spectral region.[1] In 2007, we began design and construction of a highly capable new instrument based on the Dyson principle and incorporating experience with previous dispersive hyperspectral systems.[2] The new instrument begins flight testing in September 2010.

2. OPTICS

The core of the MAKO instrument is the cryogenic Dyson spectrometer, shown in Figures 1 and 2. The spectrometer operates at f/1.25 and disperses the 7.8-13.4μm band into 128 spectral channels defined by the rows of the array. The slit length also spans 128 spatial pixels, each spatial pixel being dispersed along an array column. The additional corrector lens, a modification to the basic concentric Dyson configuration, permits greater slit and focal plane relief, necessary to package the sizable focal plane mount.

The Dyson's concave, spherical diffraction grating with 21 grooves/mm was produced by Corning Specialty Materials of Keene, New Hampshire, using advanced diamond turning processes.[3] Corning also machined the rest of the spectrometer assembly, including ZnSe Dyson lens and corrector, slit, fold mirror, and housing for the spectrometer optical elements. While fabricated and assembled at room temperature, the spectrometer is designed to come into focus and alignment at an operating temperature of 15K.[4,5,6,7,8] Because machining tolerances are small relative to the alignment budget, the only adjustments necessary are the six degrees of freedom in the focal plane mount and clocking of the slit relative to the dispersion of the grating. A diamond machined mirror and eccentric cam adjustment on the slit housing provide welcome feedback and finesse during slit clocking.

Figure 3 shows how the cryogenic optics assembly plays with the external afocal telescope in the end-to-end system. The mirrors for the external telescope are Zerodur, potted into aluminum housings with RTV. Although not athermal, the most sensitive dimension, spacing between the primary and secondary mirrors, is sufficiently insensitive to temperature change over the anticipated operating range. If necessary, titanium or even Invar metering between the primary and secondary would reduce thermal defocus. Figure 4 shows the external telescope.

*david.w.warren@aero.org; phone 1 310 336-9291; www.aero.org

Imaging Spectrometry XV, edited by Sylvia S. Shen, Paul E. Lewis, Proc. of SPIE Vol. 7812,
78120N · © 2010 SPIE · CCC code: 0277-786X/10/$18 · doi: 10.1117/12.861374

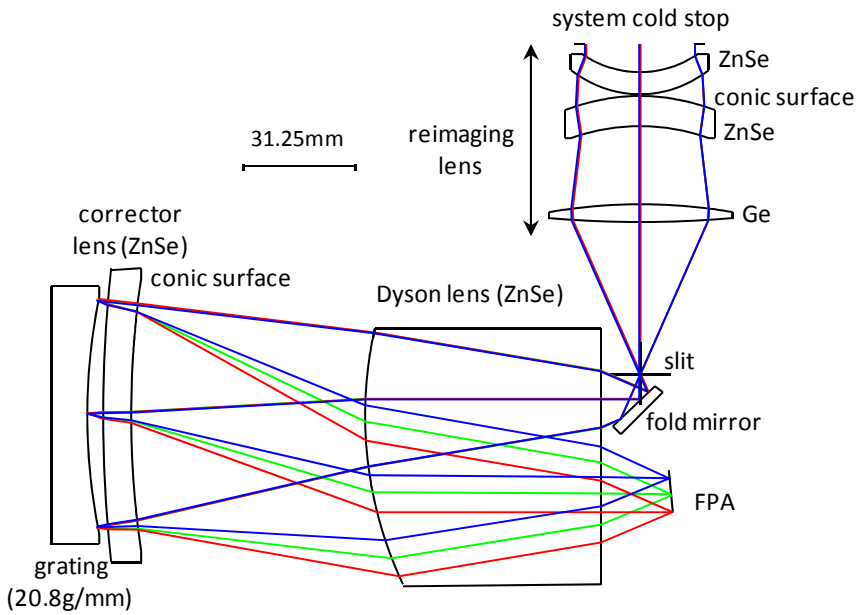

Figure 1. Raytrace detail of the MAKO cryogenic optics section. Collimated light enters the cryostat through a Zinc Selenide window (not shown). The 30mm diameter system cold stop is attached to an outer cold shroud inside the liquid helium cryostat, ensuring that the downstream optics see only cold material and walls or low emissivity mirror surfaces. A three element reimaging lens with a focal length of 37.5mm forms a telecentric image of the distant scene on the slit at a scale of 2 mrad per 75µm pixel. The Dyson spectrometer reimages and disperses the slit onto a 128x128 element Si:As focal plane operating at a temperature of 10K. The cryogenic section may be used without an external telescope as a stand-alone imager with a 14.7 degree angular swath width.

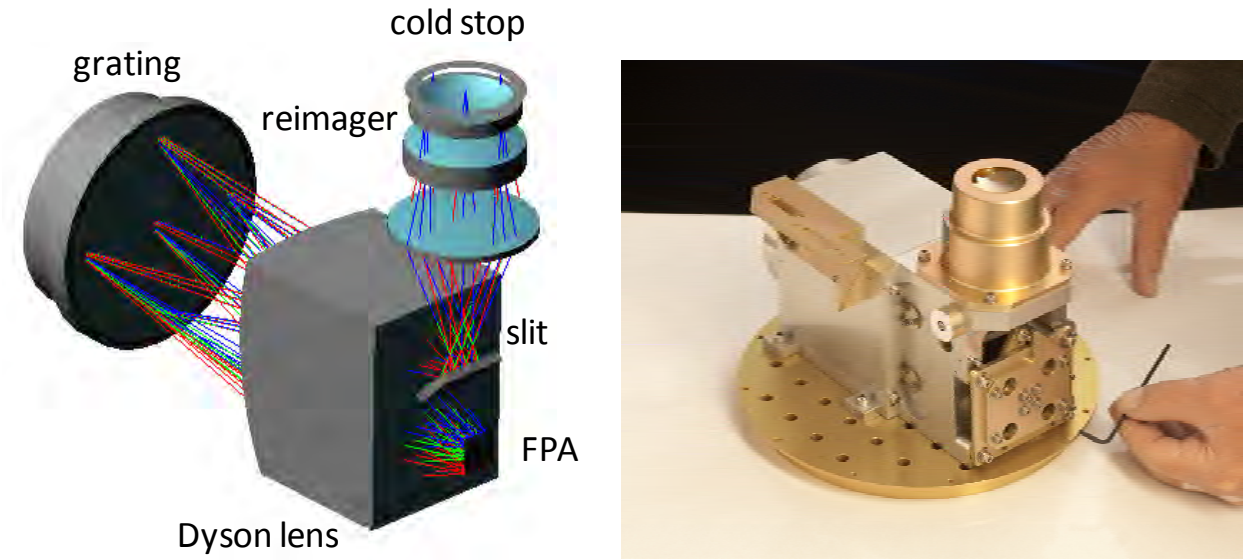

Figure 2. MAKO cryogenic optics section. Left: 3-D rendering of optical components. Right: actual hardware on the cryostat base plate. The cold stop and reimaging optics are in the gold anodized cylindrical housing at the upper right, directly above the slit. A fold mirror beneath the slit directs the optical path into the Dyson spectrometer. The corrector lens and grating are attached to the upper left end of the main housing. The focal plane mount and adjustments are at the lower right. Parts visible to the optical path are glass bead blasted and clear anodized, forming an absorbing matte finish in the LWIR.

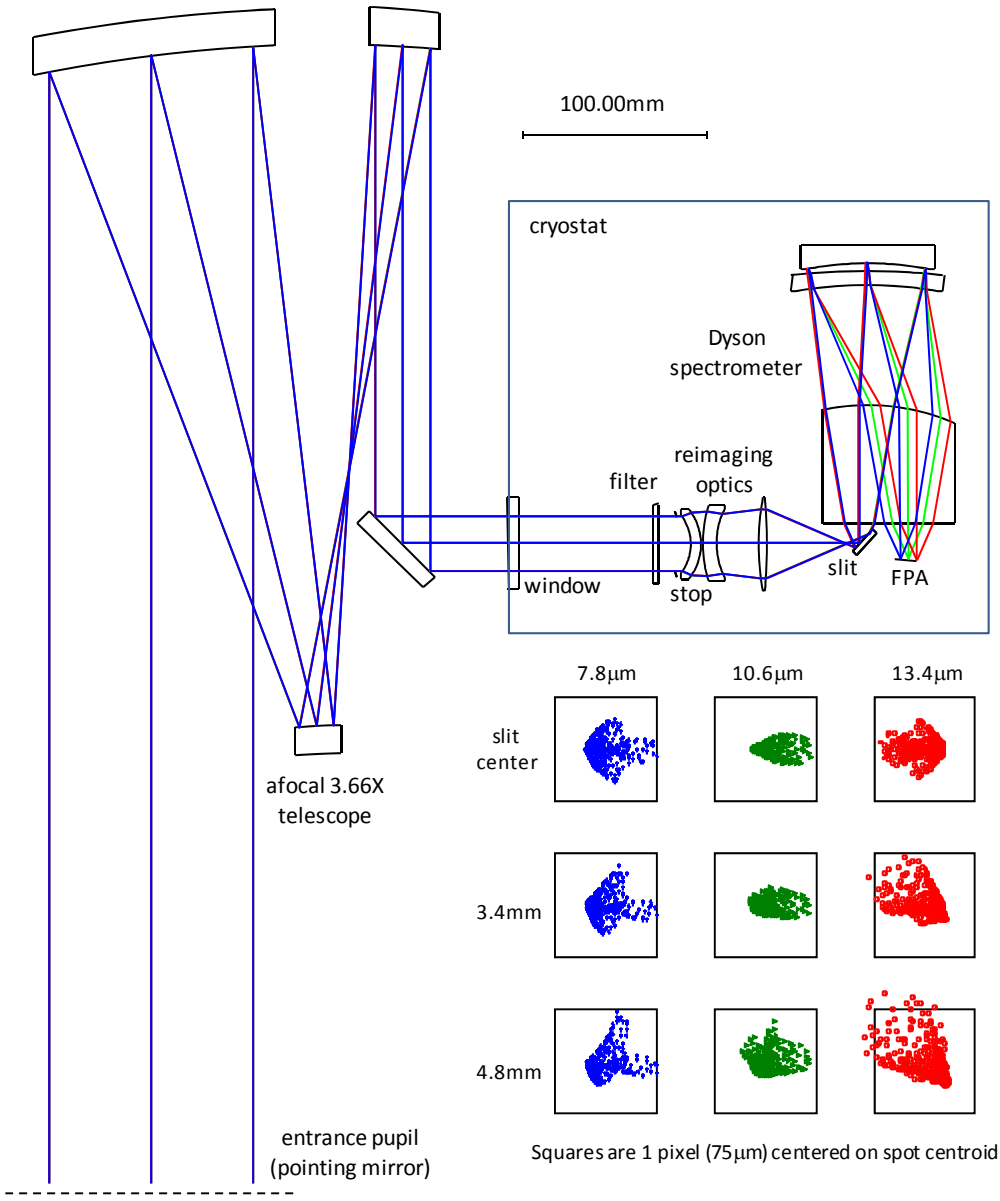

Figure 3. Raytrace layout and geometric spot images of the MAKO optical system. The afocal telescope comprises the three powered conic (paraboloid/hyperboloid/paraboloid) mirrors on the left. The cold pupil stop, reimaging optics, and spectrometer are contained in the cryostat to the right. The afocal optical interface eliminates sensitivity to defocus across the warm/cold mechanical interface. The external telescope has an angular magnification of 3.66X, reducing the 2mrad intrinsic IFOV of the cryostat optics to 547μrad, or 1 meter GSD at 6000 ft. AGL. The telescope also relays the system cold stop to an entrance pupil close to the pointing mirror, minimizing the size of the pointing mirror and black body calibration sources. End to end geometric spot diagrams for the MAKO system show good image quality with respect to the 75μm pixel dimensions, although at f/1.25, the system is not diffraction limited. Airy disk diameters range from 24 to 41μm at 7.8 and 13.4μm, respectively. Distortions are <3μm smile and <6μm keystone relative to geometric spot centroids.

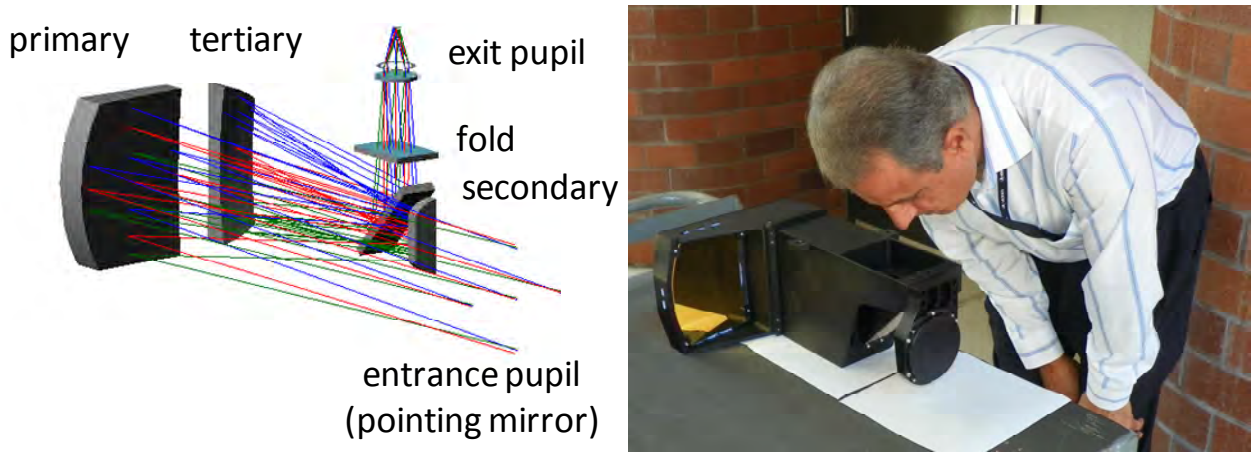

Figure 4. The MAKO external telescope. The telescope is in its flight orientation, as suspended from the underside of the spectrometer cryostat. The gold coated primary mirror is visible on the left side, surrounded by its semi-compliant RTV bonding pads. The round secondary mirror is facing the primary. Note that although only an off-center segment of the secondary is used, the full, symmetric parent secondary is mounted behind a mask. If the exposed mirror is contaminated, it can be rotated about the symmetry axis to a clean area. With the observer's eye in the exit pupil location, the telescope acts like a 4x Galilean system. The Zerodur mirrors are finished to visible surface quality.

3. POINTING AND STABILIZATION SYSTEM

The pointing and stabilization system (Figure 5) combines a commercial, gyro-stabilized aerial camera platform (Intergraph Z/I mount) to remove aircraft vibration and attitude perturbations with a custom (in-house designed and built), two-axis pointing mirror for target acquisition and scanning. Parker Automation motors with encoders and a 6K2 servo controller are used to generate the raster scans. The scanning mirror has an optical line of sight range of 90 degrees in roll and 20 degrees in pitch with a scan rate greater than 25 deg/sec, giving it a large area-coverage capability in a whiskbroom mode. There will be two principal modes of operation: high-speed, continuous area scanning (Fig. 6a) capable of covering 400 square meters/sec at 12000 feet altitude, and a slow-scan, high sensitivity, single-target mode (Fig. 6b) using a high number of sensor co-adds which increase the SNR by a factor of up to 7.

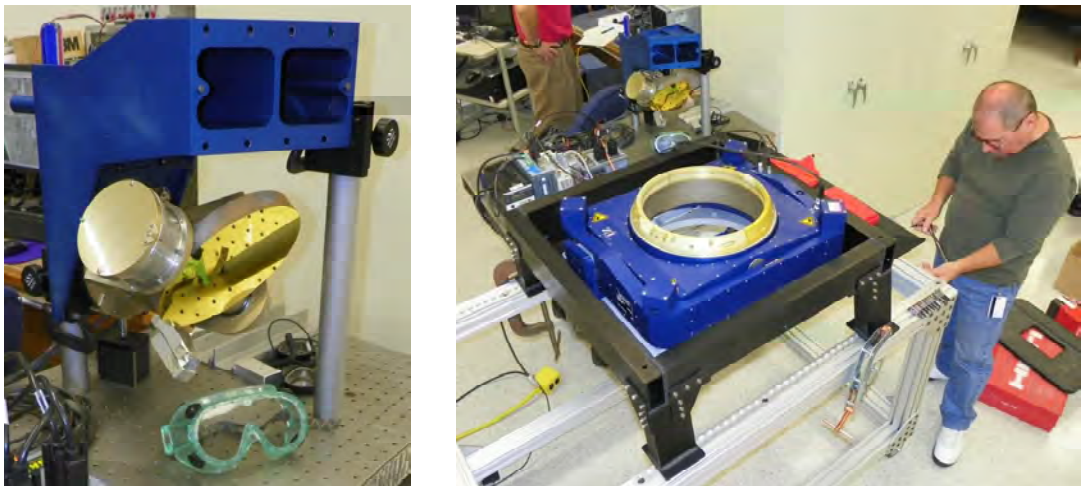

Figure 5.The MAKO pointing mirror (left) and gyro-stabilized mount (right). The stabilized mount removes aircraft attitude variations up to ±5 degrees in roll, -7 to +5 degrees in pitch, and ±30 degrees in yaw (crabbing). The pointing mirror is capable of whisking ±45 degrees in roll (cross-track) and ±10 degrees in pitch (in-track). It can also roll > ±90 degrees, in combination with a yaw of the stabilized mount, to point to the black body calibration sources (shown in Figure 10).

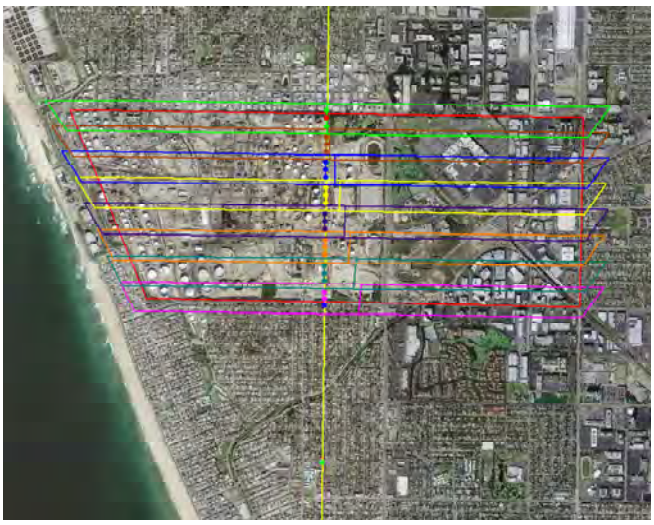

(a) Area covered: 4300 x 1600 meters (GSD = 2 m)
Altitude 12000 feet, speed 100 knots (50m/sec)
8 whisks: 1750 to 2000 frames, total 15000 frames
1 co-add, frame rate 800 Hz
Total acquisition time: 30 seconds

(b) Area covered: 800 x 256 meters (GSD = 2 m)
Altitude 12000 feet, speed 100 knots (50m/sec)
1 whisk: 400 frames,
48 co-adds @800Hz = 16.7 frames/sec
(7X SNR improvement over 1 co-add)
Total acquisition time: 24 seconds

Figure 6. Simulations of two extreme collection scenarios showing the mission planning feature of the Otter flight software program. The image on the left shows maximum area coverage rate, with a sawtooth whisk of ±45 degrees every 4 seconds as the aircraft/stabilized mount flies straight and level. MAKO can keep up with this area coverage rate indefinitely, limited only by the size of the RAID storage. Note the slit rotation off-nadir, as shown by the ends of the whisks. The image on the right shows a maximum signal/noise collect, with the pointing mirror pitch axis compensating for aircraft forward motion during a single, slow, crosstrack scan.

4. ELECTRONICS AND DATA SYSTEM

Fig. 7 is a block diagram of the electronics and software subsystems. The entire system is controlled by a single computer with 2 quad-core processors hosting multi-threaded sensor control, data-acquisition, targeting, and navigation software. Graphical user interfaces (Fig. 8) are used to control the sensor, monitor status, display real-time focal-plane and waterfall images, and display quick-look images of whisks acquired (Fig 9).

Data from the focal plane are digitized with 16 channels of A/D converters, acquired with a Dalsa X64 Xcelera frame grabber, and will ultimately be recorded at up to a 4KHz frame rate to a RAID disk subsystem at 64 Mpixels/sec. Sensor location is recorded from a Novatel differential GPS at 20 Hz with a 2 meter accuracy, and absolute line of sight (LOS) measurements at 64 Hz are obtained using a Litton 100G inertial navigation unit attached to the optical bench on the cryostat (see Figure 10). Angle data from three KVH DSP-3000 fiber optic gyros are recorded at 200 Hz to refine the attitude knowledge, and high-precision encoders on the mirror axes are recorded to determine sensor line of sight. All data are time-tagged using an external GPS clock source, enabling geolocation accuracy to several meters.

The computer also hosts the in-house developed moving-map and flight-line-following navigation software (called "Otter") which can be used for real-time mission planning and sensor tasking. It is possible to lay out an area on the ground, automatically fill it with whisks, and send the targeting commands to the sensor control process in under a minute. The system will be flexible enough to cover multiple areas and acquire widely-dispersed single targets on a flight line.

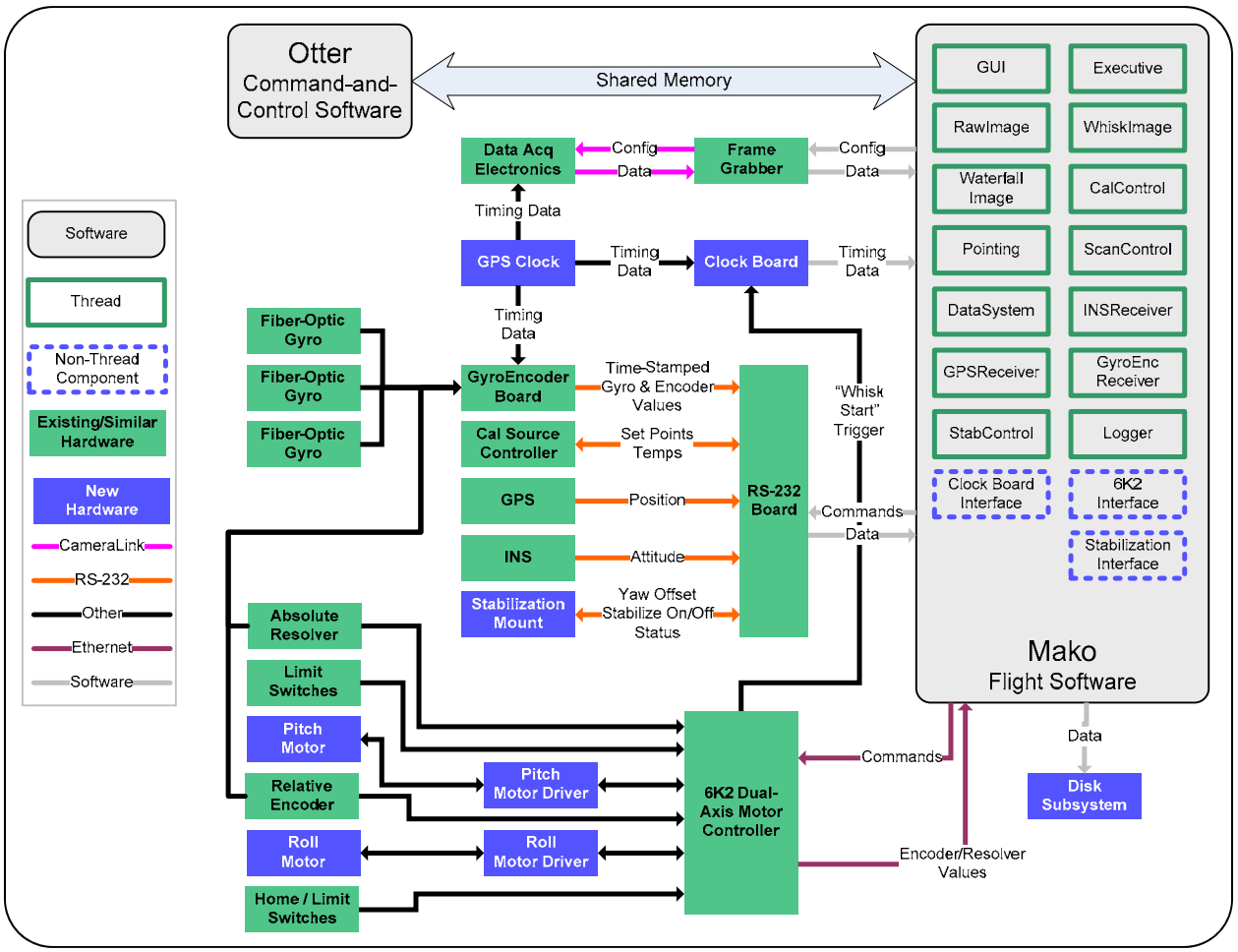

Figure 7. Control and data paths in the MAKO system.

5. INITIAL RESULTS

Figure 10 shows the complete MAKO system nearly ready for installation in the Twin Otter aircraft. Figures 11 and 12 show spectral and spatial performance of the new system after one focus iteration. First light axial focus (determined with a modified Hartmann procedure using the shift in centroid of a spectral feature with illumination position in the sensor pupil) was off about 0.28mm at the focal plane, resulting in about a 4 pixel blur. This was remarkably good considering the system is f/1.25 and was adjusted at room temperature based on predictions of mechanical and refractive index changes when cooled to 20K. As much as anything, this is a testament to the refractive index models published by the CHARMS facility at NASA Goddard.[4] Based on experience with previous cryogenic sensors, we expect adjustments to converge on optimized performance within 3 iterations.

6. FUTURE PLANS

Flight testing on the Twin Otter is scheduled to begin in September of 2010. Before, during, and after the flights, we will continue to refine optical end electronic adjustments in order to maximize and characterize spectral and spatial performance.

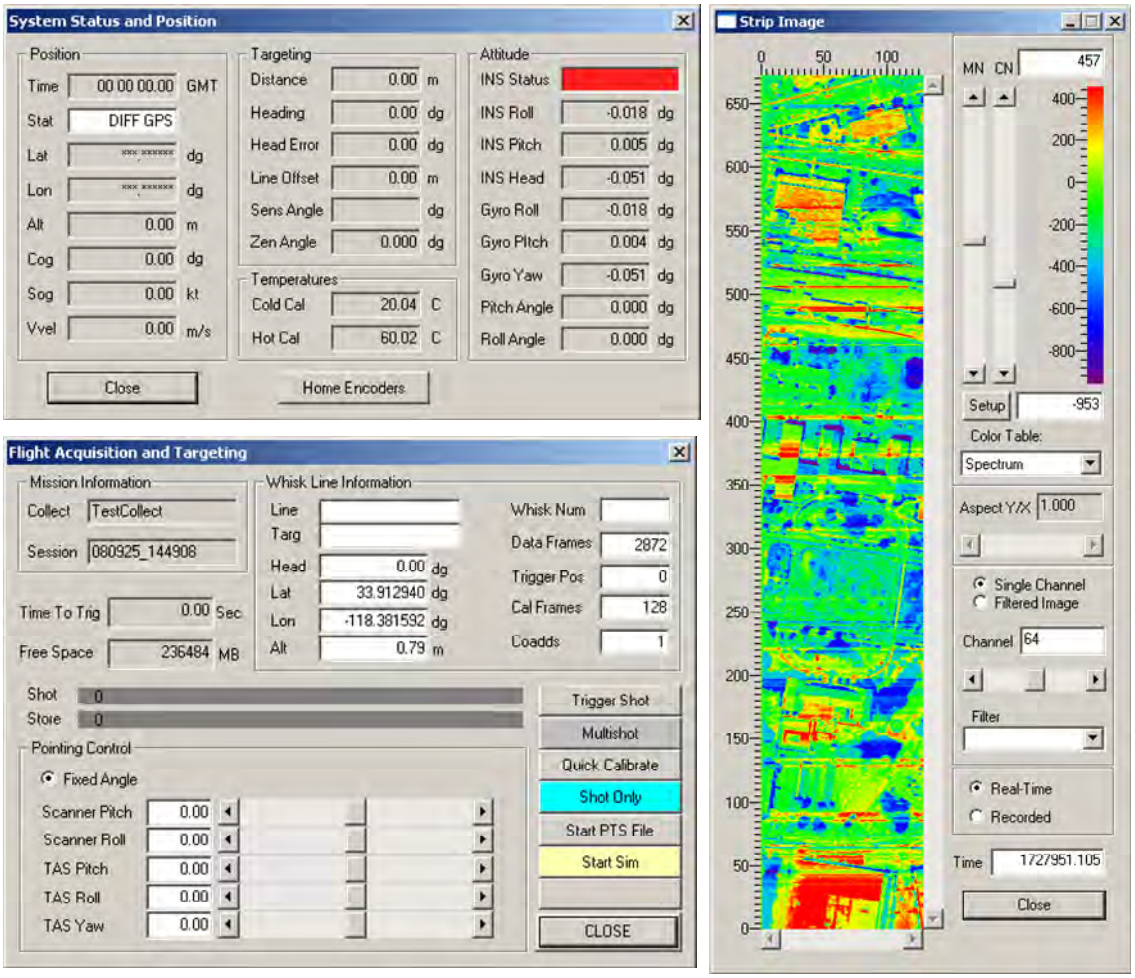

Figure 8. Typical sensor control and monitoring GUIs. The waterfall display at right shows the real-time sensor data (simulated image).

Figure 9. Display Whisk Image window, showing the images acquired for each whisk (simulated images).

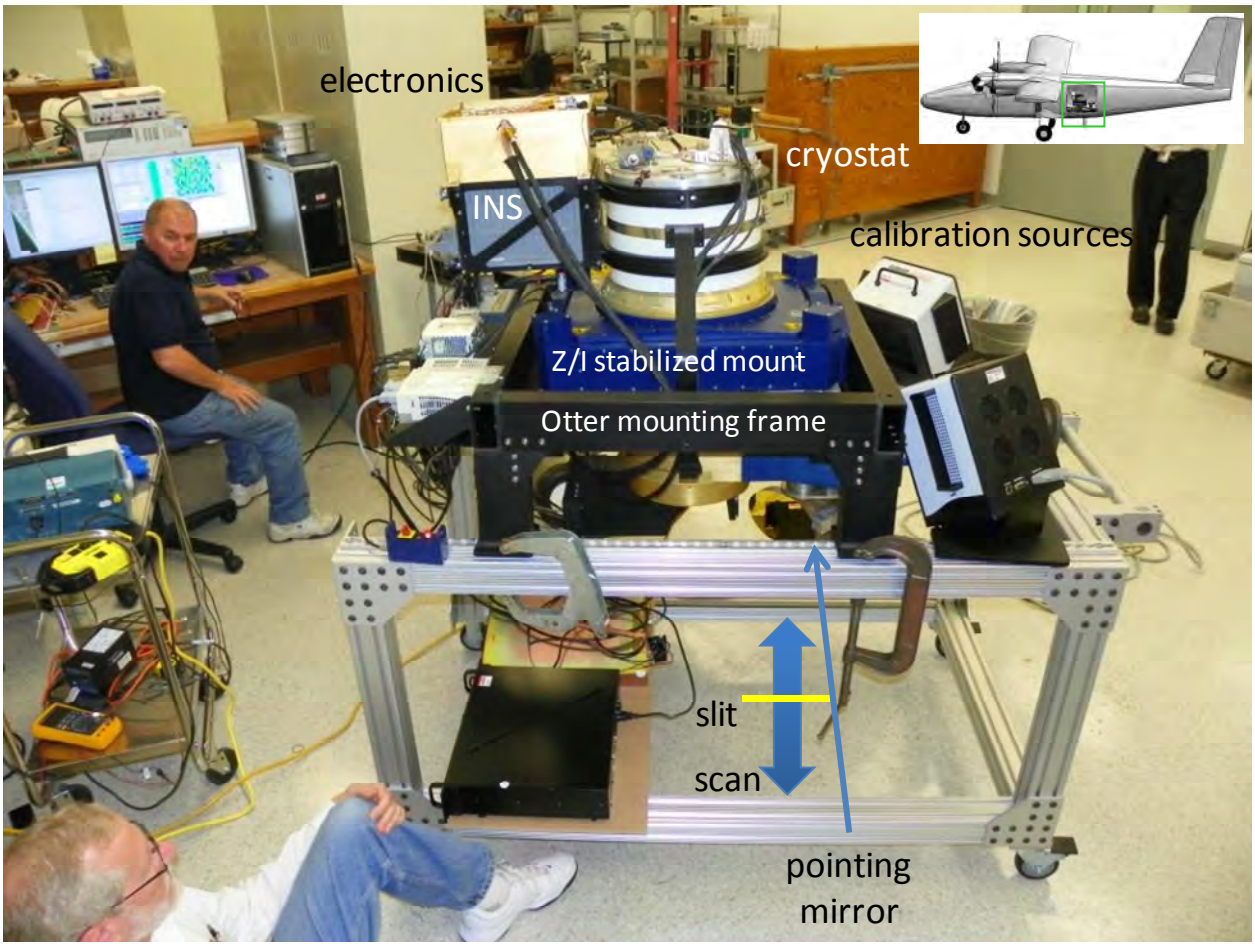

Figure 10. The MAKO system in the flight configuration. Left is towards the front of the aircraft. The entire unit is designed to be picked up by the black mounting frame and lifted into the Otter cabin, where it bolts to standard seat rails straddling the camera port. The total lifted weight is about 380 pounds..

ACKNOWLEDGEMENTS

This work was supported under The Aerospace Corporation's Corporate Research Initiative Program.

The MAKO project was conceived and initiated by John Hackwell.

Precision Aspheres of Fremont, California did a superb job figuring the external telescope mirrors.

Corning Specialty Materials of Keene, New Hampshire did their usual excellent work in fabricating the diamond machined diffraction grating and Dyson spectrometer assembly.

The underlying images in Figure 6 are from the USGS via the Microsoft Research Maps Project.

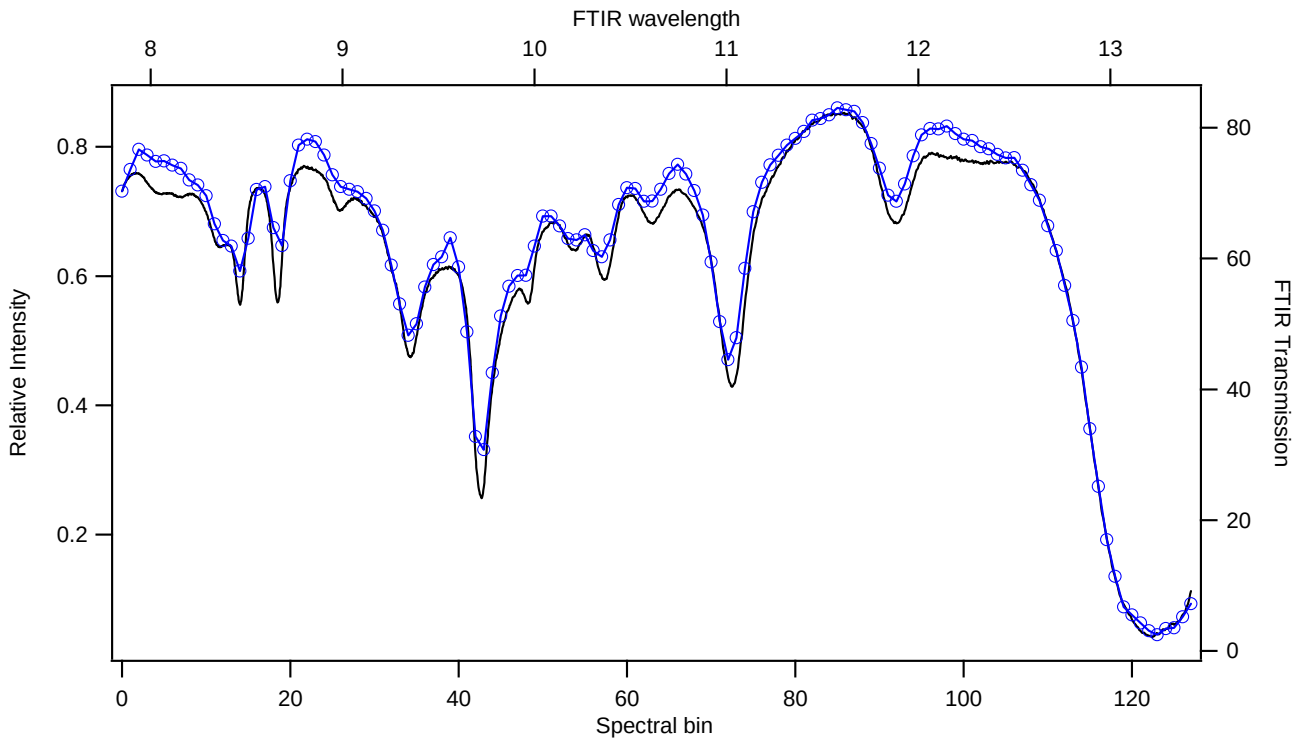

Figure 11. Spectrum of NIST Standard Reference Material 1921a polystyrene film after one focal plane axial focus iteration. The solid black line is a FTIR spectrum of the film at 0.5 wavenumber resolution. The blue circles and fitted blue line are data from each of the 128 spectral channels covering 7.8 – 13.4μm (536 wavenumbers). One MAKO spectral bin should therefore be about 4 wavenumbers.

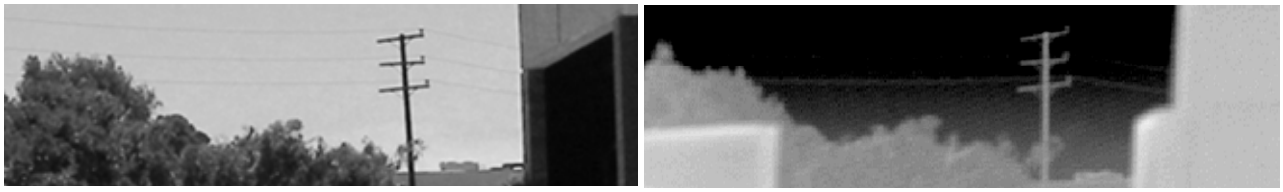

Figure 12. Visible panchromatic still image (left) and 10.6μm scanned image (right). The pointing mirror is rolled out 90 degrees (horizontal) so the slit is vertical. Horizontal scanning is then accomplished with the pitch axis of the pointing mirror. At the finite range (<100m) of the trees and utility pole, their images will be at least 3 pixels out of focus with the system focused for an infinite object distance.

REFERENCES

[1] Warren, D. W., D. J. Gutierrez, and E. R. Keim, "Dyson spectrometers for high-performance infrared applications," Optical Engineering, 47, 103601-1-9, (2008).

[2] Hackwell, J. A.,*et al*, "LWIR/MWIR Imaging hyperspectral sensor for airborne and ground-based remote sensing," Proc. SPIE 2819, 102-107 (1996).

[3] Cobb, J. M., "Advances in diamond turned surfaces enable unique cost-effective optical system solutions," Proc. SPIE 6269, 62691L-1-9 (2006)

[4] Leviton, D. B., B. J. Frey, and T. Kvamme, "High accuracy, absolute, cryogenic refractive index measurements of infrared lens materials for JWST NIRCam using CHARMS," Proc. SPIE 5904, 59040O-1-12 (2005)

[5] W.J. Tropf, "Temperature-dependent refractive index models for BaF2, CaF2, MgF2, SrF2, LiF, NaF, KCl, ZnS, and ZnSe," Optical Engineering, 34, 1369-1373 (1995)

[6] Hoffman, J. M. and W. L. Wolfe, "Cryogenic refractive indices of ZnSe, Ge, and Si at 10.6μm," Applied Optics, 30, 4014-4016 (1991)

[7] NIST Thermophysical Properties Division, Cryogenics Technologies Group web site: http://cryogenics.nist.gov

[8] Touloukian, Y. S., *Thermophysical Properties of Matter*, John Wiley & Sons, New York, (1970)